Low-Cost Battery Monitoring by Converter-Based Electrochemical Impedance Spectroscopy

R. Ferrero, C. Wu
Dept. of Electrical Engineering and Electronics
University of Liverpool, Liverpool, UK
Email: Roberto.Ferrero@liverpool.ac.uk
C.Wu15@liverpool.ac.uk

M. De Angelis, H. George-Williams, E. Patelli
Institute for Risk and Uncertainty
University of Liverpool, Liverpool, UK
Email: Marco.De-Angelis@liverpool.ac.uk
H.George-Williams@liverpool.ac.uk
Edoardo.Patelli@liverpool.ac.uk

A. Carboni, S. Toscani
Dip. di Elettronica, Informazione e Bioingegneria
Politecnico di Milano, Milano, Italy
Email: alberto.carboni@polimi.it
sergio.toscani@polimi.it

P. Pegoraro
Department of Electrical and Electronic Engineering
University of Cagliari, Cagliari, Italy
Email: paolo.pegoraro@diee.unica.it

***Abstract*—The use of batteries and other electrochemical devices in modern power systems is rapidly increasing, with stricter requirements in terms of cost, efficiency and reliability. Innovative monitoring solutions are therefore urged to allow a successful development of a wide range of emerging applications, including electric vehicles and large-scale energy storage to support renewable energy generation. Presently, a huge gap still exists between the accurate and sophisticated monitoring techniques commonly employed in laboratory tests, on the one hand, and the simple and rough solutions available in commercial applications, on the other hand. The objective of this paper is therefore to demonstrate how measurements similar to those performed in laboratories can be carried out also in commercial applications at very low cost. In more detail, the paper focuses on electrochemical impedance spectroscopy on a battery, performed by a DC-DC power converter suitably controlled to create the required AC perturbation, and it explains how the converter control, the signal acquisition and advanced processing and estimation algorithms can all be implemented in low-cost off-the-shelf hardware, capable to achieve very accurate results. The paper mainly presents the design of the complete system and describes the experimental prototype used to test the proposed methodology.**

***Index Terms*—Batteries, Battery management systems, Electrochemical devices, Electrochemical impedance spectroscopy, Condition monitoring, State estimation, DC-DC power converters**

I. Introduction

Batteries and more generally electrochemical power sources are playing an increasingly important role in modern power systems, driven by the wider use of renewable energy and allowed by the recent developments in electrochemical technology [1]. Battery use is no longer limited to low-power devices, as many emerging applications nowadays include large-scale energy storage for renewable energy generation and powertrain for electric or hybrid vehicles, just to mention a few examples.

Despite the impressive advancements in battery technology in recent years, further improvements are still much needed in key aspects for commercial applications, namely efficiency, reliability and cost. While most of the efforts toward such improvements are focused on battery design and material technology, in-situ monitoring systems also play a very important role. In fact, a more accurate state estimation of the battery internal conditions would allow, on the one hand, a better power management (therefore higher overall efficiency of the power system) and, on the other hand, a more accurate and prompter diagnosis of performance degradation processes (therefore a more reliable operation). If all this were achieved at negligible additional instrumentation cost, the decrease in the overall operation and maintenance costs would lead also to large economic benefits.

Electrochemical impedance spectroscopy (EIS) is a very powerful non-invasive measurement technique, commonly employed in laboratory experiments, which provides a wealth of diagnostic information about electrochemical processes occurring within batteries (and fuel cells as well). The main advantage compared to DC voltage and current measurements alone is that EIS allows distinguishing between different processes and different causes of voltage drop, as they affect the impedance spectrum in different frequency ranges, from millihertz to kilohertz [2]. Several works in the literature have demonstrated how EIS can be effectively employed to accurately estimate the battery state of charge (SOC) and state of health (SOH) [2]–[6]. Nevertheless, to the best knowledge of the Authors, EIS is not presently employed for in-situ condition monitoring in commercial applications, as the expensive and sophisticated instrumentation used in the laboratory (such as frequency response analyzers) is not affordable in those applications. Typically, only DC voltages and currents are monitored, on individual cells or on groups of cells, but in any case with limited capability of providing accurate and reliable

information about the state of the battery, particularly the SOH.

The use of power converters has been recently suggested as a possible solution to achieve EIS in commercial applications at lower cost. Indeed, power converters represent a very promising solution because they are already available in most applications and, if properly controlled, they can introduce AC perturbations superimposed to the battery DC current and voltage, at the desired frequencies to measure the impedance spectrum in relevant frequency ranges. This solution would not require any additional hardware to create the AC perturbations, although may require additional hardware to implement the necessary advanced features for the power converter control and to acquire and process the current and voltage measurements.

A number of papers have appeared in the literature in the last few years, reporting the results of preliminary feasibility studies applied to batteries [7]–[10], as well as to fuel cells [11]–[13]. The solutions presented in the literature so far are, however, still affected by important limitations, mainly arising from the need to find a balance between high accuracy of results, on the one hand, and the use of simple and inexpensive hardware, on the other hand. In the simplest solution [7], the voltage and current signals are processed in the time domain, by measuring their peak-to-peak amplitudes and the time delay between the two waveforms, which leads to much less accurate results compared to a frequency-domain analysis in presence of noise or distortions. Even when the signals are processed in the frequency domain, the AC perturbation is often just a sine wave and allows measuring the impedance at one frequency at a time [8], [9], whereas a multi-sine perturbation would be very useful to dramatically decrease the measurement time and obtain more accurate impedance spectra. Moreover, the perturbations are added by modulating the converter duty cycle by a sinusoidal oscillation, instead of directly controlling the battery current or voltage, and this may lead to significant distortions in the waveforms. On the other hand, when the battery current or voltage are directly controlled and more advanced signal processing is added to identify model parameters from full impedance spectra, a simple DSP can no longer cope with the computational burden, and more complex hardware is required, together with external software tools such as Matlab [10].

The objective and new contribution of this paper are therefore the design of a fully embedded solution for converter control, signal acquisition and advanced signal processing, entirely based on a low-cost off-the-shelf hardware platform that combines hard-real time signal generation and acquisition with the processing capability of a modern computer. Such a solution has the potential to allow not only impedance measurements, but also accurate SOC and SOH estimation by means of advanced model identification and uncertainty analysis.

II. Battery SOC and SOH Estimation by EIS

The battery state and behavior are characterized by the interplay of a large number of physical processes, occurring on very different time scales, from microseconds to years [2]. EIS measurements can typically cover a frequency range down to millihertz or slightly below, therefore the impedance spectrum includes the effects of three main processes, namely ohmic phenomena (in the kilohertz range), charge transfer in the electrochemical double layer (in the hertz range) and mass transport of ions (in the millihertz range). Fig. 1 shows the Nyquist diagram of a typical spectrum, where the three phenomena above can be clearly distinguished.

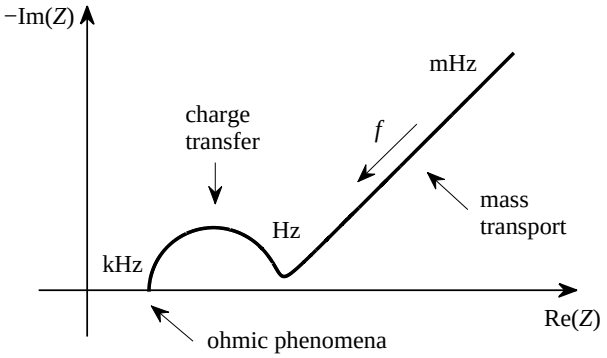

Fig. 1. Typical impedance spectrum of a battery, in a frequency range from millihertz to kilohertz, revealing different electrochemical processes.

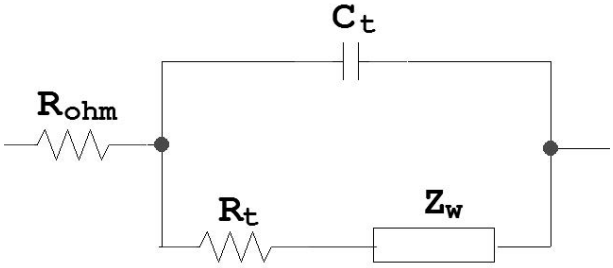

Fig. 2. Equivalent circuit of the battery impedance, corresponding to the impedance spectrum shown in Fig. 1.

The impedance spectrum can be interpreted in terms of an equivalent electrical circuit, where each impedance is associated with a different process and represents a different contribution to the overall voltage drop (and losses, in case of resistive components). Several equivalent circuits can be found in the literature, of different type and complexity, used to model different batteries in different conditions, but a simple and common circuit approximately valid for all battery types is illustrated in Fig. 2, where R_{ohm} represents the ohmic losses, R_{t} and C_{t} represent the charge double layer, and Z_{w} (called Warburg impedance) represents the mass transport and is defined by the following expression:

$$Z_{\mathrm{w}}(j\omega) = \sigma_{\mathrm{w}} \frac{1-j}{\sqrt{\omega}} \tag{1}$$

Processes occurring on longer time scales, such as those due to a change in the SOC or due to aging (deterioration of SOH) can be detected as changes in the values and shape of

the spectrum and can be interpreted in terms of changes in one or more of the equivalent circuit parameters, although the relationship may not always be straightforward. In lithium-ion batteries, the SOC does not significantly affect the ohmic resistance while it mainly affects the mass transport and, to a lower extent, the charge transfer [2]–[4], whereas in lead-acid batteries the SOC affects also the ohmic resistance [6]; in both battery types, however, the main variations are visible in the low-frequency part of the impedance spectrum. On the other hand, the SOH affects the whole spectrum, at high and low frequencies, in both lithium-ion [2], [3] and lead-acid [6] batteries, with different parts of the spectrum being more or less influenced by different causes of performance degradation and aging.

The use of EIS to accurately estimate the battery SOC and SOH requires therefore the measurement of the impedance spectrum in a wide frequency range, down to the millihertz region, thus with a very long measurement time which is extremely challenging, particularly in commercial applications, because the battery is unlikely to remain in steady-state conditions during such a long time. For this reason, a classic Fourier approach may lead to highly inaccurate results, and more sophisticated algorithms combining time-domain and frequency-domain analysis should be used to compensate for changes in the operating conditions or internal state of the battery [14]. Implementing such algorithms in commercial applications at low cost is an important challenge, and the aim of this paper is to present a possible hardware platform to address this challenge.

III. Hardware Design and Experimental Setup

A. DC-DC Boost Converter

The proposed methodology is tested on a switch-mode DC-DC boost converter, as batteries are low-voltage, high-current sources and in most applications their voltage has to be boosted to match the load requirements or to decrease the energy transmission losses. A converter prototype was specifically designed and assembled for this purpose, instead of using a commercial product, in order to have a full control over the converter and be able to customize the switch control strategy according to the aim of the paper.

The equivalent circuit of the whole power system, composed of source, converter and load, is illustrated in Fig. 3, while a photograph of the prototype is shown in Fig. 4. The chosen battery is a 12 V, 7 Ah sealed lead-acid battery composed of 6 cells in series, and the boost converter was designed for a primary (battery) rated current of 10 A. A variable resistor with 10 Ω maximum resistance is used as the load for sake of simplicity. Because of the low power of the circuit, the controlled switch is a MOSFET, and the converter was designed to operate with pulse width modulation (PWM) control at switching frequencies between 10 kHz and 100 kHz. The board also includes a LEM LA 25-P closed-loop Hall-effect current transducer, with a frequency bandwidth from 0 to 200 kHz, used to measure the battery current.

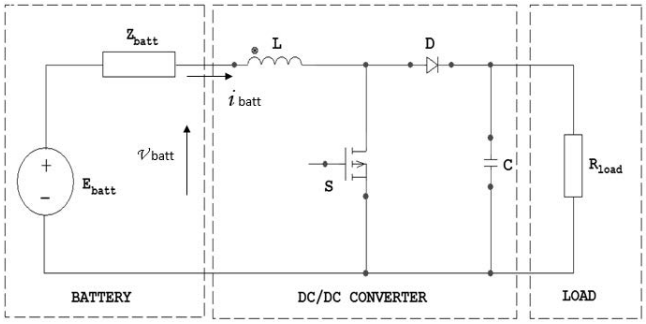

Fig. 3. Equivalent circuit of the designed power system prototype, composed of a battery (with its impedance that has to be measured), a DC-DC boost converter and a resistive load.

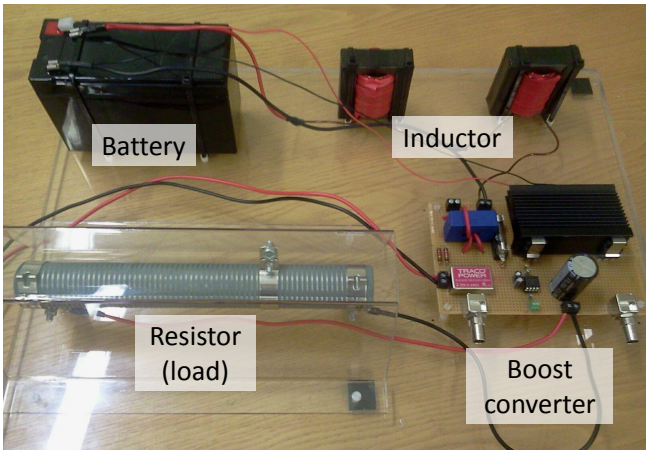

Fig. 4. Photograph of the prototype used for the tests, composed of a lead-acid battery, a home-made DC-DC converter and a resistive load.

When the converter operates in continuous conduction mode, the ideal (without losses) relationship between input and output voltages is:

$$V_{\mathrm{o}} = \frac{V_{\mathrm{i}}}{1-\delta} \tag{2}$$

where V_{i} and V_{o} are the DC (or slowly changing, compared to the switching period) voltages and δ is the converter duty cycle, i.e. the fraction of the switching period when the switch is on. The switching frequency f_{sw} and duty cycle δ affect also the peak-to-peak amplitudes of the input current ripple ΔI_{i} and output voltage ripple ΔV_{o}, and the consequent design of the input inductance L and output capacitance C. Again, in ideal conditions, the following equations are derived, respectively:

$$\Delta I_{\mathrm{i}} = \frac{V_{\mathrm{i}}\delta}{L f_{\mathrm{sw}}} \tag{3}$$

$$\Delta V_{\mathrm{o}} = \frac{I_{\mathrm{i}}\,(1-\delta)\,\delta}{C f_{\mathrm{sw}}} \tag{4}$$

Based on (3) and on the rated input voltage (12 V) and current (10 A), an inductance L = 1.2 mH was chosen to guarantee a peak-to-peak input current ripple below 10% of the DC current at f_{sw} = 10 kHz and below 1% at f_{sw} = 100 kHz.

Similarly, based on (4), a capacitance C = 470 μF was chosen to guarantee a peak-to-peak output voltage below 3% of the DC voltage at f_{sw} = 10 kHz and below 0.3% at f_{sw} = 100 kHz.

The switch control, described in the next subsection, allows controlling the duty cycle on time scales of tens of microseconds, in order to introduce AC perturbations at frequencies up to a few kilohertz, depending on the chosen switching frequency. This converter is therefore suitable to measure the full impedance spectrum of the battery, as illustrated in the previous section.

B. Signal Acquisition, Generation and Processing

The hardware required to implement the proposed impedance measurement technique must have hard real-time processing capability, to control the converter operation and to acquire the voltage and current measurement signals, and at the same time it must have a large computational power to implement signal processing and state estimation algorithms in order to calculate the impedance spectrum and identify model parameters from it, possibly with an estimation of the uncertainty associated with them to assess the accuracy and reliability of the determined SOC and SOH. Last but not least, such hardware should be also simple, inexpensive and compact, in order to be easily applied to commercial applications, and flexible enough to be customized to accommodate different measurement requirements in terms of accuracy, number of channels, etc.

According to these considerations, a BeagleBone Black (BBB) board, shown in Fig. 5, appears to be an appropriate choice. The BBB is a low-cost (around $50) development board that includes a Texas Instruments 1-GHz AM3358 ARM Cortex-A8 processor (supporting several open-source operating systems, such as Linux), as well as 2 separate 200-MHz programmable real-time units (PRUs), sharing the same data bus with the ARM processor, thus allowing a simple and fast exchange of data. The BBB features a number of digital input-output channels, including PWM outputs suitable for the converter switch control. The board also includes an 8-channel, 12-bit, 200-kSa/s analog-to-digital converter (ADC), which is suitable to acquire the battery voltage and current signals with appropriate sampling frequency and resolution. If, however, a particular application requires (and can afford) more accurate measurements or more channels, it is possible to add external ADCs to the board, connected through a serial interface (SPI), with a limited cost increase. Similarly, if a larger computational power or more advanced graphical visualization are required, a Raspberry Pi board (featuring a Quad-Core ARM Cortex-A53 processor) can be easily connected to the BBB, with the overall cost still being within $100.

A schematic diagram of the proposed system for signal acquisition, generation and processing is illustrated in Fig. 6. The voltage and current signals contain a large DC component and a much smaller AC component; therefore the two components are firstly separated by low-pass and high-pass filters and then attenuated/amplified as appropriate in order to match the input voltage range of the ADC. It is

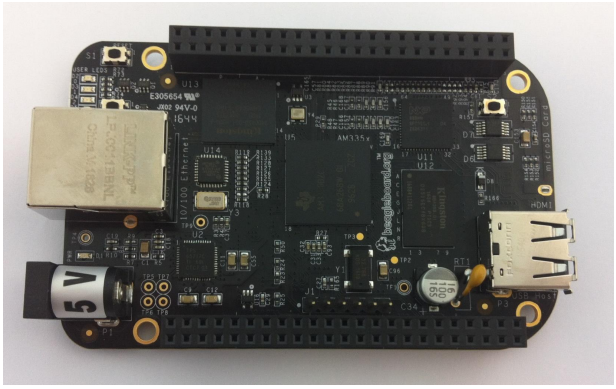

Fig. 5. Photograph of the BeagleBone Black board, which is chosen as the hardware platform for the implementation of signal acquisition, generation and processing, according to the aim of the paper.

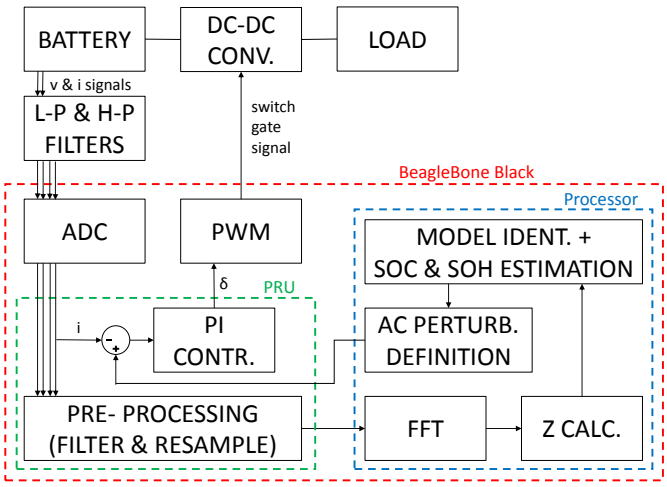

Fig. 6. Schematic diagram of the PWM signal generation and voltage and current signal acquisition and processing, based on the BeagleBone Black board.

worth noting that the AC perturbation may go down to the millihertz range, so separating the DC from such a low-frequency AC component is a challenging task. The digital current value is then compared to a pre-defined reference signal, and a PI controller calculates the required duty cycle for the power converter to follow such reference. The controller is implemented in the BBB PRU, which also manages the analog inputs and PWM output of the board in hard real-time. Depending on the frequency of the AC perturbation, the PRU will also implement a moving average filter and will down-sample the signals in order to limit the data sent to the processor. The data will be temporarily stored in a memory buffer, waiting to be read by the processor, whose operation is not hard real-time but is fast enough to allow reading the buffer before it is overwritten.

The processor will then calculate the Fourier Transform of the voltage and current signals, after having compensated for any variation of the operating condition during the measurement (necessary at very low frequencies), and will determine

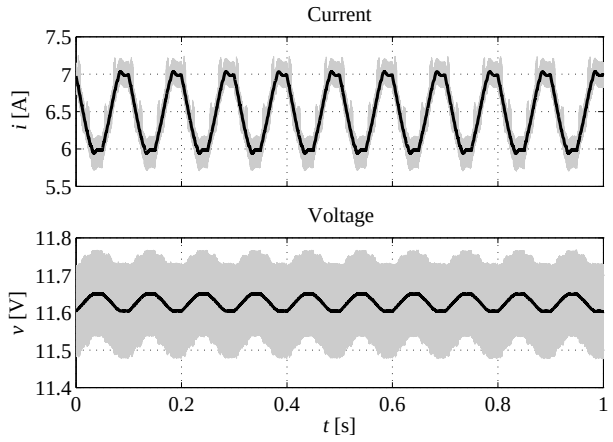

Fig. 7. Example of battery current (upper plot) and voltage (lower plot) obtained by modulating the converter duty cycle with a 10 Hz oscillation, when the converter is operated at 10 kHz switching frequency; the light-gray lines represent the original waveforms and the thicker black lines represent the signals averaged over the switching period.

the impedance spectrum of the battery. Suitable model parameters will then be identified based on the measured spectrum, in order to detect variations in the SOC or SOH. An estimation of the uncertainty of those parameters is also necessary, in order to assess the reliability of any detected change in the SOC or SOH.

IV. Preliminary Experimental Results

The software implementation in the BBB is still in progress, and complete results showing the measurement of full impedance spectra and variations of the battery SOC and SOH estimated by them will be reported in the final version of the paper. Here, only the results of preliminary tests carried out on the boost converter prototype are reported, to demonstrate how AC perturbations can be introduced by modulating the duty cycle of the converter switch.

As an example. Fig. 7 shows the battery current perturbed by a 10 Hz oscillation around 6.5 A, together with the voltage response to such a perturbation. The 10 Hz oscillation is well visible once the higher-frequency perturbation caused by the converter switching (at 10 kHz in this case) and the high-frequency noise are removed by averaging the signals over the switching period (0.1 ms). By applying the Fourier Transform and calculating the ratio between the voltage and current spectra, the impedance at 10 Hz is calculated, which results to be 44-j4 mΩ. Similarly, impedance values at other frequencies can be calculated. In order to keep the measurement time as low as possible, in the final implementation a multi-sine signal containing 10 frequencies in a decade will be used instead of a sine wave.

V. Conclusions

This paper described a low-cost hardware platform suitable to perform in-situ electrochemical impedance spectroscopy on batteries employed in commercial applications, by using the already available DC-DC converter to introduce AC perturbations superimposed to the DC current and voltage, at the desired frequencies in a wide range from millihertz to kilohertz. A BeagleBone Black board was shown to be an appropriate hardware solution to control the converter, acquire and process the current and voltage measurements, and estimate the battery SOC and SOH based on the impedance spectrum, because it combines hard real-time programmable units with a powerful processor, and its cost and size are likely to be affordable in a commercial application.

The design of the hardware (including the power converter) and preliminary measurements results were reported. Complete results including full impedance spectra and the variations in the battery SOC and SOH estimated from them will be added in the final version of the paper.

References

[1] X. Luo, J. Wang, M. Dooner and J. Clarke, "Overview of current development in electrical energy storage technologies and the application potential in power system operation", *Applied Energy*, vol. 137, pp. 511-536, 2015.

[2] A. Jossen, "Fundamentals of battery dynamics", *Journal of Power Sources*, vol. 154, pp. 530-538, 2006.

[3] W. Waag, S. Käbitz and D. U. Sauer, "Experimental investigation of the lithium-ion battery impedance characteristic at various conditions and aging states and its influence on the application", *Applied Energy*, vol. 102, pp. 885-897, 2013.

[4] D. Andre, M. Meiler, K. Steiner, Ch. Wimmer, T. Soczka-Guth and D. U. Sauer, "Characterization of high-power lithium-ion batteries by electrochemical impedance spectroscopy. I. Experimental investigation", *Journal of Power Sources*, vol. 196, pp. 5334-5341, 2011.

[5] U. Tröltzsch, O. Kanoun and H.-R. Tränkler, "Characterizing aging effects of lithium ion batteries by impedance spectroscopy", *Electrochimica Acta*, vol. 51, pp. 1664-1672, 2006.

[6] F. Huet, "A review of impedance measurements for determination of the state-of-charge or state-of-health of secondary batteries", *Journal of Power Sources*, vol. 70, pp. 59-69, 1998.

[7] W. Huang and J. A. Abu Qahouq, "An online battery impedance measurement method using DC-DC power converter control", *IEEE Trans. on Industrial Electronics*, vol. 61, no. 11, pp. 5987-5995, 2014.

[8] A. Densmore and M. Hanif, "Determining battery SoC using electrochemical impedance spectroscopy and the extreme learning machine", *IEEE 2nd Int. Future Energy Electronics Conference*, Taipei, Taiwan, 1-4 Nov. 2015, pp. 1-7.

[9] M. A. Varnosfaderani and D. Strickland, "Online impedance spectroscopy estimation of a battery", *18th European Conference on Power Electronics and Applications*, Karlsruhe, Germany, 5-9 Sep. 2016, pp. 1-10.

[10] E. Din, C. Schaef, K. Moffat and J. T. Stauth, "A scalable active battery management system with embedded real-time electrochemical impedance spectroscopy", *IEEE Trans. on Power Electronics*, vol. 32, no. 7, pp. 5688-5698, 2017.

[11] G. Dotelli, R. Ferrero, P. Gallo Stampino, S. Latorrata and S. Toscani, "PEM fuel cell drying and flooding diagnosis with signals injected by a power converter", *IEEE Trans. on Instrumentation and Measurement*, vol. 64, no. 8, pp. 2064-2071, 2015.

[12] G. Dotelli, R. Ferrero, P. Gallo Stampino, S. Latorrata and S. Toscani, "Low-cost PEM fuel cell diagnosis based on power converter ripple with hysteresis control", *IEEE Trans. on Instrumentation and Measurement*, vol. 64, no. 11, pp. 2900-2907, 2015.

[13] N. Katayama and S. Kogoshi, "Real-time electrochemical impedance diagnosis for fuel cells using a DC-DC converter", *IEEE Trans. on Energy Conversion*, vol. 30, no. 2, pp. 707-713, 2015.

[14] G. Dotelli, R. Ferrero, P. Gallo Stampino and S. Latorrata, "Analysis and compensation of PEM fuel cell instabilities in low-frequency EIS measurements", *IEEE Trans. on Instrumentation and Measurement*, vol. 63, no. 7, pp. 1693-1700, 2014.